Available online at www.sciencedirect.com

ScienceDirect

Optics Communications 281 (2008) 1–6

OPTICS COMMUNICATIONS

www.elsevier.com/locate/optcom

A cascade of singular field patterns in Young's interference experiment

T.D. Visser [a,*], R.W. Schoonover [b]

[a] Department of Physics and Astronomy, Free University, De Boelelaan 1081, 1081 HV Amsterdam, The Netherlands
[b] Department of Electrical and Computer Engineering, University of Illinois at Urbana-Champaign, 405 N. Mathews, Urbana, IL 61801, USA

Received 15 June 2007; received in revised form 21 August 2007; accepted 31 August 2007

Abstract

We analyze Young's interference experiment for the case that two correlated, linearly polarized beams are used. It is shown that even when the incident fields are partially coherent, there are always correlation singularities (pairs of lines where the fields are completely uncorrelated) on the observation screen. These correlation singularities evolve in a non-trivial manner into dark lines (phase singularities in the paraxial approximation). The latter in turn each unfold into a triplet of polarization singularities, namely an L-line and two C-lines of opposite handedness.

1. Introduction

More than two centuries after its conception, Thomas Young's interference experiment [1–3] remains a source of novel insights. Several new effects have been predicted [4,5] or observed [6,7]. Also, so-called correlation singularities [8–11], pairs of points at which the fields are completely uncorrelated, have been identified in Young's interference pattern [12]. Several recent studies are concerned with the state of polarization of the field [13–15]. This aspect allows the study of a new kind of singular behavior [16]. Everywhere in a monochromatic field, the end-point of the electric vector traces out an ellipse over time. This polarization ellipse is characterized by three parameters describing its eccentricity, orientation and handedness. Polarization singularities [17–24], points where the ellipse has degenerated into a circle (so-called C-points, where the orientation of the ellipse is undefined) or into a line (so-called L-points, where the handedness is undefined), have, to the best of our knowledge, never been charted in the context of Young's experiment.

It has recently become apparent that different types of optical singularities are connected [25]. In the present paper, the relation between correlation singularities, dark lines, and polarization singularities is discussed. It is shown how each of them may occur in Young's double-slit experiment. Also, the continuous evolution of correlation singularities into dark lines and their subsequent unfolding into polarization singularities is described. This is done by analyzing the field that results from the superposition of two correlated beams with identical linear polarization. By gradually increasing the state of coherence of the two beams until they are fully coherent and co-phasal, pairs of correlation singularities are shown to transform into pairs of dark lines. If then the two directions of polarization are changed in a continuous manner from being parallel to making a finite angle with each other, each dark line is found to unfold into a pair of C-lines of opposite handedness plus an L-line. A possible experimental realization of this 'cascade' of field patterns is proposed.

2. Correlation singularities and dark lines

Consider a plane, opaque screen $\mathscr{A}$ with two identical, small apertures located at $Q_1(\mathbf{r}'_1)$ and $Q_2(\mathbf{r}'_2)$, that are

* Corresponding author. Tel.: +31 20 598 7864; fax: +31 20 598 7899.
E-mail address: tvisser@nat.vu.nl (T.D. Visser).

0030-4018/$ - see front matter © 2007 Elsevier B.V. All rights reserved.
doi:10.1016/j.optcom.2007.08.068

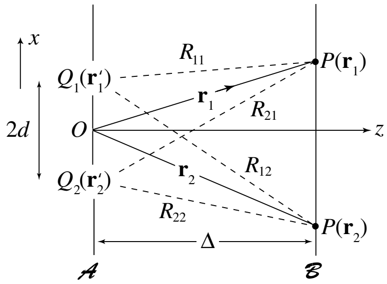

Fig. 1. Illustrating the notation.

separated by a distance $2d$ (see Fig. 1). At each aperture a linearly polarized beam is incident. The two beams are partially coherent, and their directions of polarization are for now taken to be parallel. The latter assumption allows us to use scalar diffraction theory. An interference pattern is formed on a second screen $\mathscr{B}$ that is parallel to $\mathscr{A}$ and a distance Δ away from it. Let

$$\mathbf{r}'_1 = (d,0,0) \quad \mathbf{r}'_2 = (-d,0,0), \tag{1}$$

and let the two incident fields at frequency ω be given by $U^{(\mathrm{inc})}(\mathbf{r}'_1,\omega)$ and $U^{(\mathrm{inc})}(\mathbf{r}'_2,\omega)$. The second-order coherence properties of the incident fields may be characterized by the cross-spectral density function [26], i.e.

$$W^{(\mathrm{inc})}(\mathbf{r}'_1,\mathbf{r}'_2;\omega) = \langle U^{(\mathrm{inc})*}(\mathbf{r}'_1,\omega)U^{(\mathrm{inc})}(\mathbf{r}'_2,\omega)\rangle, \tag{2}$$

where the angle brackets denote averaging over an ensemble of field realizations. The spectral degree of coherence is the normalized version of the cross-spectral density function, viz.

$$\mu_{12}^{(\mathrm{inc})}(\omega) = \frac{W^{(\mathrm{inc})}(\mathbf{r}'_1,\mathbf{r}'_2;\omega)}{\sqrt{S^{(\mathrm{inc})}(\mathbf{r}'_1,\omega)S^{(\mathrm{inc})}(\mathbf{r}'_2,\omega)}}, \tag{3}$$

where

$$S^{(\mathrm{inc})}(\mathbf{r}'_i,\omega) = W^{(\mathrm{inc})}(\mathbf{r}'_i,\mathbf{r}'_i;\omega), \quad (i=1,2) \tag{4}$$

is the spectral density of the field at pinhole i. We assume the two spectral densities to be equal, i.e. $S^{(\mathrm{inc})}(\mathbf{r}'_1,\omega) = S^{(\mathrm{inc})}(\mathbf{r}'_2,\omega) = S^{(\mathrm{inc})}(\omega)$.

It can be shown that the modulus of the spectral degree of coherence is bounded:

$$0 \leqslant \left|\mu_{12}^{(\mathrm{inc})}(\omega)\right| \leqslant 1. \tag{5}$$

The lower bound corresponds to completely uncorrelated light, whereas the upper bound corresponds to fully coherent light. For all intermediate values the light is said to be partially coherent.

The field at two observation points $P(\mathbf{r}_1)$ and $P(\mathbf{r}_2)$ on screen $\mathscr{B}$ is, assuming small angles of incidence and diffraction, given by the formulae [3, Sec. 8.8]

$$U(\mathbf{r}_1,\omega) = K_{11}U^{(\mathrm{inc})}(\mathbf{r}'_1,\omega) + K_{21}U^{(\mathrm{inc})}(\mathbf{r}'_2,\omega), \tag{6}$$

$$U(\mathbf{r}_2,\omega) = K_{12}U^{(\mathrm{inc})}(\mathbf{r}'_1,\omega) + K_{22}U^{(\mathrm{inc})}(\mathbf{r}'_2,\omega), \tag{7}$$

where

$$K_{ij} = -\frac{i}{\lambda}\mathrm{d}\mathscr{A}\frac{\mathrm{e}^{\mathrm{i}kR_{ij}}}{R_{ij}}, \quad (i,j=1,2) \tag{8}$$

and $\mathrm{d}\mathscr{A}$ denotes the area of each pinhole, R_{ij} the distance Q_iP_j and $k = 2\pi/\lambda = \omega/c$ is the wavenumber associated with frequency ω, λ being the wavelength and c the speed of light.

It is convenient to use the customary paraxial approximations [3, Sec.8.8.1] for the factors K_{ij}, viz.

$$K_{1j} \approx -\frac{\mathrm{i}\mathrm{d}\mathscr{A}}{\lambda R_{1j}}\mathrm{e}^{\mathrm{i}kR_j}\mathrm{e}^{-\mathrm{i}k\mathbf{r}'_1\cdot\hat{\mathbf{r}}_j} \approx -\frac{\mathrm{i}\mathrm{d}\mathscr{A}}{\lambda\Delta}\mathrm{e}^{\mathrm{i}kR_j}\mathrm{e}^{-\mathrm{i}kdx_j/\Delta}, \tag{9}$$

$$K_{2j} \approx -\frac{\mathrm{i}\mathrm{d}\mathscr{A}}{\lambda R_{2j}}\mathrm{e}^{\mathrm{i}kR_j}\mathrm{e}^{-\mathrm{i}k\mathbf{r}'_2\cdot\hat{\mathbf{r}}_j} \approx -\frac{\mathrm{i}\mathrm{d}\mathscr{A}}{\lambda\Delta}\mathrm{e}^{\mathrm{i}kR_j}\mathrm{e}^{\mathrm{i}kdx_j/\Delta}, \tag{10}$$

where $\mathbf{r}_j = (x_j,y_j,z_j)$, $R_j = |\mathbf{r}_j|$ and $\hat{\mathbf{r}}_j = \mathbf{r}_j/R$. It is to be noted that the vector products appearing in Eqs. (9) and (10) imply that the observed field is, in the vicinity of the x-axis, essentially invariant in the direction perpendicular to the line connecting the two pinholes, i.e. in the y-direction. We will therefore restrict our analysis to observation points along the x-axis. It should be noted however, that the field behavior we discuss occurs along lines.

The cross-spectral density function of the field on screen $\mathscr{B}$ is defined, strictly analogous to Eq. (2), as

$$W(\mathbf{r}_1,\mathbf{r}_2;\omega) = \langle U^*(\mathbf{r}_1,\omega)U(\mathbf{r}_2,\omega)\rangle, \tag{11}$$

with its spectral degree of coherence given by the expression

$$\mu(\mathbf{r}_1,\mathbf{r}_2;\omega) = \frac{W(\mathbf{r}_1,\mathbf{r}_2;\omega)}{\sqrt{S(\mathbf{r}_1,\omega)S(\mathbf{r}_2,\omega)}}, \tag{12}$$

where $S(\mathbf{r}_i,\omega) = W(\mathbf{r}_i,\mathbf{r}_i;\omega)$ is the spectral density at $P(\mathbf{r}_i)$. The modulus of the spectral degree of coherence of the field on the observation screen is again bounded, i.e.

$$0 \leqslant |\mu(\mathbf{r}_1,\mathbf{r}_2;\omega)| \leqslant 1, \tag{13}$$

with the bounds having the same meaning as for $\mu_{12}^{(\mathrm{inc})}(\omega)$.

As mentioned before, we consider observation points that lie on the x-axis. As a further specialization, we will analyze pairs of points that are located symmetrically with respect to the z-axis, i.e. we take

$$\mathbf{r}_1 = (x,0,\Delta), \tag{14}$$

$$\mathbf{r}_2 = (-x,0,\Delta). \tag{15}$$

On substituting from Eqs. (6) and (7) into Eq. (11) while using the approximations (9) and (10) we then obtain for the spectral density and the cross-spectral density the expressions

$$S(\mathbf{r}_1,\omega) = 2\left(\frac{\mathrm{d}\mathscr{A}}{\lambda\Delta}\right)^2 S^{(\mathrm{inc})}(\omega)\left\{1+\left|\mu_{12}^{(\mathrm{inc})}(\omega)\right|\cos(\beta+2k\mathrm{d}x/\Delta)\right\}, \tag{16}$$

$$S(\mathbf{r}_2,\omega) = 2\left(\frac{\mathrm{d}\mathscr{A}}{\lambda\Delta}\right)^2 S^{(\mathrm{inc})}(\omega)\left\{1+\left|\mu_{12}^{(\mathrm{inc})}(\omega)\right|\cos(\beta-2k\mathrm{d}x/\Delta)\right\}, \tag{17}$$

$$W(\mathbf{r}_1,\mathbf{r}_2;\omega)=2\left(\frac{\mathrm{d}\mathscr{A}}{\lambda\Delta}\right)^2 S^{(\mathrm{inc})}(\omega)\left\{\Re[\mu_{12}^{(\mathrm{inc})}(\omega)]+\cos(2k\mathrm{d}x/\Delta)\right\}, \tag{18}$$

where β denotes the argument (phase) of $\mu_{12}^{(\mathrm{inc})}(\omega)$. We note that $S(\mathbf{r}_1,\omega) \neq S(\mathbf{r}_2,\omega)$ because, in general, $\mu_{12}^{(\mathrm{inc})}(\omega) \neq \mu_{21}^{(\mathrm{inc})}(\omega)$.

As is well known, there are no observation points where the spectral density vanishes when Young's experiment is performed using partially coherent light. (However, this is not necessarily true when three partially coherent beams are made to interfere. [27–29]) In the present case this follows from the fact that $|\mu_{12}^{(\mathrm{inc})}(\omega)| < 1$ for partially coherent light, and therefore the terms in braces in Eqs. (16) and (17) have no zeros.

It is seen from Eqs. (16) and (17) that in the limit $\Re[\mu_{12}^{(\mathrm{inc})}(\omega)] \to 1$, i.e. when the two incident fields are fully coherent and co-phasal, the spectral density vanishes at points

$$\mathbf{r} = (x_n, 0, \Delta), \tag{19}$$

where

$$x_n = \pm\frac{\pi\Delta}{kd}(n+1/2), \quad (n = 0,1,2,\ldots) \tag{20}$$

It is to be noted that the complete destructive interference that leads to the spectral density to be zero at these points is a direct consequence of the use of the paraxial approximation [Eqs. (9) and (10)]. In reality, rather than phase singularities, there will be dark lines on the observation screen with a vanishing but non-zero intensity.

In contrast to the field amplitude, the behavior of the correlation functions is more subtle. There are pairs of observation points at which the fields are completely incoherent (i.e. pairs of points for which $W(\mathbf{r}_1,\mathbf{r}_2;\omega) = \mu(\mathbf{r}_1,\mathbf{r}_2;\omega) = 0$) even if the incident is partially coherent. A necessary and sufficient condition for this to occur is for the term in braces in Eq. (18) to become zero, i.e

$$\cos(2k\mathrm{d}x/\Delta) = -\Re[\mu_{12}^{(\mathrm{inc})}(\omega)]. \tag{21}$$

In view of the relation (5) it follows that Eq. (21) can always be satisfied. So we conclude that even if the two incident fields are partially coherent, there are pairs of observation points $\mathbf{r}_1 = (x,0,\Delta)$, $\mathbf{r}_2 = (-x,0,\Delta)$ at which the fields at frequency ω are completely uncorrelated. Let us now examine the behavior of the solutions of Eq. (21) for the case that $\Re[\mu_{12}^{(\mathrm{inc})}(\omega)]$ is positive. We can write the positive solutions for the position x as

$$x_n^{\pm} = \frac{\pi\Delta}{kd}(\pm\delta + n + 1/2), \quad (n = 0,1,2,\ldots), \tag{22}$$

with δ a positive constant that depends on the value of $\Re[\mu_{12}^{(\mathrm{inc})}(\omega)]$, and the superscript $\pm$ indicating whether the plus or minus sign is taken in front of δ. If $\Re[\mu_{12}^{(\mathrm{inc})}(\omega)]$ tends to unity, δ becomes smaller and the points x_n^+ and x_n^-, that are each part of two different correlation singularities, namely the pairs of points $(-x_n^+, x_n^+)$ and $(-x_n^-, x_n^-)$, move closer to each other. In the limit of the two incident fields becoming fully coherent and co-phasal, the points x_n^+ and x_n^- merge and both correlation singularities disappear, i.e.

$$\lim_{\Re[\mu_{12}^{(\mathrm{inc})}(\omega)]\to 1} x_n^+ = x_n^- = x_n. \tag{23}$$

In this limit the points $\pm x_n^{\pm}$ become the dark lines given by Eq. (19). Hence, we conclude that in the limit of the two incident fields becoming fully coherent and co-phasal (i.e. $\mu_{12}^{(\mathrm{inc})}(\omega) = 1$), each half of the correlation singularity $(-x_n^+, x_n^+)$ annihilates with a neighboring half of the correlation singularity $(-x_n^-, x_n^-)$. The result of this 'cross-pair' annihilation of correlation singularities is a dark line at x_n. (Only in the idealized paraxial case are these dark lines true zeros of intensity, i.e. phase singularities.)

An example is shown in Fig. 2 in which four coherence singularities (i.e. four pairs of points) are shown for selected values of the real part of the spectral degree of coherence, $\Re[\mu_{12}^{(\mathrm{inc})}(\omega)]$. In panel (a) the equally-colored pairs $(-x_0^-, x_0^-)$, $(-x_0^+, x_0^+)$, $(-x_1^-, x_1^-)$ and $(-x_1^+, x_1^+)$ each form a coherence singularity, in other words $\mu(-x_0^-, x_0^-; \omega) = \mu(-x_0^+, x_0^+; \omega) = \mu(-x_1^-, x_1^-; \omega) = \mu(-x_1^+, x_1^+; \omega) = 0$. In panel b, the same four coherence singularities are shown for a higher value of $\Re[\mu_{12}^{(\mathrm{inc})}(\omega)]$. It is seen that each half of a correlation singularity, like e.g. x_0^-, moves closer to a neighboring half of another correlation singularity, in this case x_0^+. In panel c, the limiting case of $\Re[\mu_{12}^{(\mathrm{inc})}(\omega)] = 1$ is

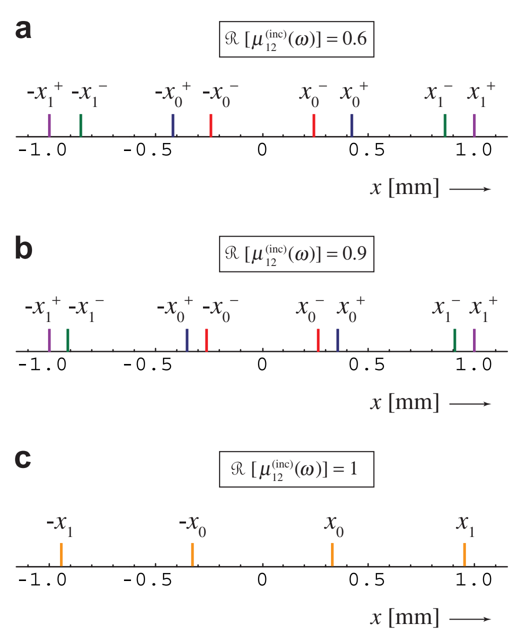

Fig. 2. The position of four correlation singularities, i.e. the pairs of observation points $(-x_1^+, x_1^+)$, $(-x_1^-, x_1^-)$, $(-x_0^+, x_0^+)$, and $(-x_0^-, x_0^-)$ at which the fields are completely uncorrelated, for selected values of $\Re[\mu_{12}^{(\mathrm{inc})}(\omega)]$. The pairs are indicated by equally-colored bars. In panels (a) and (b) it is seen how each half of a singularity moves towards a neighboring half. In panel (c) the incident fields are fully coherent and co-phasal. The four correlation singularities have annihilated and four dark lines have been created at $-x_1$, $-x_0$, x_0, and x_1. In this example $\lambda = 632.8$ nm, $\Delta = 2$ m, and $2d = 2$ mm.

shown. Now the four correlation singularities have annihilated, and four dark lines at $-x_1$, $-x_0$, x_0, and x_1 have been created.

3. Dark lines and polarization singularities

In order to study polarization effects, we must use a vector description rather than the scalar description we used thus far. The incident fields are assumed to be fully coherent and linearly polarized. The two angles of polarization are under an angle α with each other. Let the electric fields at frequency ω that are incident on the two pinholes be given by the expressions

$$\mathbf{E}(\mathbf{r}_1', \omega) = E\exp(-\mathrm{i}\omega t)\hat{\mathbf{x}}, \tag{24}$$

$$\mathbf{E}(\mathbf{r}_2', \omega) = E\exp(-\mathrm{i}\omega t)[\cos\alpha\hat{\mathbf{x}} + \sin\alpha\hat{\mathbf{y}}], \tag{25}$$

where t denotes the time, and $\hat{\mathbf{x}}$ and $\hat{\mathbf{y}}$ are unit vectors in the x and y-direction, respectively, and $E \in \mathbb{R}$. The electric field at an observation point $P(\mathbf{r})$ is then, again assuming small angles of incidence and diffraction, given by the formula

$$\mathbf{E}(\mathbf{r}, \omega) = K_1\mathbf{E}(\mathbf{r}_1', \omega) + K_2\mathbf{E}(\mathbf{r}_2', \omega), \tag{26}$$

with

$$K_1 = -\frac{i}{\lambda}\mathrm{d}\mathscr{A}\frac{\mathrm{e}^{\mathrm{i}k|\mathbf{r}-\mathbf{r}_1'|}}{|\mathbf{r}-\mathbf{r}_1'|} \approx -\frac{i\mathrm{d}\mathscr{A}}{\lambda\Delta}\mathrm{e}^{\mathrm{i}kR}\mathrm{e}^{-\mathrm{i}k\mathrm{d}x/\Delta}, \tag{27}$$

$$K_2 = -\frac{i}{\lambda}\mathrm{d}\mathscr{A}\frac{\mathrm{e}^{\mathrm{i}k|\mathbf{r}-\mathbf{r}_2'|}}{|\mathbf{r}-\mathbf{r}_2'|} \approx -\frac{i\mathrm{d}\mathscr{A}}{\lambda\Delta}\mathrm{e}^{\mathrm{i}kR}\mathrm{e}^{\mathrm{i}k\mathrm{d}x/\Delta}, \tag{28}$$

where $\mathbf{r} = (x,y,\Delta)$, and $R = |\mathbf{r}|$. On substituting from Eqs. (24) and (25) into Eq. (26) while using the approximations (27) and (28), we obtain for the field on the screen the expression

$$\mathbf{E}(\mathbf{r}, \omega) = -i\frac{E\mathrm{d}\mathscr{A}}{\lambda\Delta}\mathrm{e}^{\mathrm{i}(kR-\omega t)}[(\mathrm{e}^{-\mathrm{i}k\mathrm{d}x/\Delta} + \cos\alpha\mathrm{e}^{\mathrm{i}k\mathrm{d}x/\Delta})\hat{\mathbf{x}} + \sin\alpha\mathrm{e}^{\mathrm{i}k\mathrm{d}x/\Delta}\hat{\mathbf{y}}]. \tag{29}$$

If we define

$$a_1 = |E_x(\mathbf{r}, \omega)|, \quad a_2 = |E_y(\mathbf{r}, \omega)|, \tag{30}$$

$$\delta_1 = \arg E_x(\mathbf{r}, \omega), \quad \delta_2 = \arg E_y(\mathbf{r}, \omega), \tag{31}$$

then the Stokes parameters that characterize the state of polarization of the field at $P(\mathbf{r})$ can be expressed as [3]

$$S_0 = a_1^2 + a_2^2, \quad S_1 = a_1^2 - a_2^2, \tag{32}$$

$$S_2 = 2a_1a_2\cos\delta, \quad S_3 = 2a_1a_2\sin\delta, \tag{33}$$

where $\delta = \delta_2 - \delta_1$. The first parameter, S_0, is proportional to the intensity of the field. The normalized Stokes vector (s_1,s_2,s_3), with $s_i = S_i/S_0$ and $i = 1,2,3$, indicates a point on the Poincaré sphere. The north pole ($s_3 = 1$) and south pole ($s_3 = -1$) correspond to circular polarization. Points on the equator ($s_3 = 0$) correspond to linear polarization. All other points correspond to elliptical polarization. At points above the equator ($s_3 > 0$) the polarization is right-handed, whereas as at points below the equator ($s_3 < 0$) the polarization is left-handed. The smallest angle between the major axis of the polarization ellipse and the positive x-axis equals

$$\Psi = \frac{1}{2}\arctan\left(\frac{s_2}{s_1}\right). \tag{34}$$

Let us now study the behavior of the Stokes parameters in the vicinity of a dark line (with near-zero intensity) that occurs when the two directions of polarization are parallel, i.e. when $\alpha = 0$. In that case, the field everywhere is linearly polarized along the x-direction ($s_1 = 1$, $s_2 = s_3 = 0$). This situation is depicted in Fig. 3a and b. Also, according to Eqs. (32) and (29),

$$S_0 = \left[\frac{2E\mathrm{d}\mathscr{A}}{\lambda\Delta}\cos(k\mathrm{d}x/\Delta)\right]^2. \tag{35}$$

Hence, we find as before that (albeit it only in the paraxial approximation) the intensity vanishes at the points x_n given by Eq. (20). If we consider the field around the point x_0 and apply a Taylor expansion to Eq. (29) for small values of the angle α, we find that

$$E_x(x_0, \omega) = 0, \tag{36}$$

$$E_y(x_0, \omega) = i\frac{\alpha E\mathrm{d}\mathscr{A}}{\lambda\Delta}. \tag{37}$$

Hence, on changing α from zero to a finite value, the x-component of the electric field remains approximately zero, whereas the y-component obtains a finite imaginary value. Thus, the dark line at x_0 evolves into a polarization singularity, namely an L-line with $s_1 = -1$. We also note that the first term in the square brackets of Eq. (29) is approximately real near x_0, whereas the second term is approximately imaginary. That implies that the Stokes parameter s_2, remains unaffected, i.e. close to zero, under small changes in the angle α. To study the behavior of the parameter s_3, it is useful to expand the electric field given by Eq. (29) in the circular polarization basis [30] as

$$\begin{aligned} e_\pm(\mathbf{r}, \omega) &= -i\frac{E\mathrm{d}\mathscr{A}}{\lambda\Delta\sqrt{2}}\mathrm{e}^{\mathrm{i}(kR-\omega t)} \\ &\quad \times \left[\mathrm{e}^{-\mathrm{i}k\mathrm{d}x/\Delta} + \cos\alpha\mathrm{e}^{\mathrm{i}k\mathrm{d}x/\Delta} \mp i\sin\alpha\mathrm{e}^{\mathrm{i}k\mathrm{d}x/\Delta}\right] && (38) \\ &= -i\frac{E\mathrm{d}\mathscr{A}}{\lambda\Delta\sqrt{2}}\mathrm{e}^{\mathrm{i}(kR-\omega t)}\left[\mathrm{e}^{\mathrm{i}k\mathrm{d}x/\Delta}e^{\mp\mathrm{i}\alpha} + \mathrm{e}^{-\mathrm{i}k\mathrm{d}x/\Delta}\right], && (39) \end{aligned}$$

where e_+ and e_- are the amplitudes for the left-handed and right-handed circular polarization basis, respectively. The zeros of these quantities occur when

$$k\mathrm{d}x_\pm/\Delta \mp \alpha = -k\mathrm{d}x_\pm/\Delta + \pi, \tag{40}$$

i.e. at positions

$$x_\pm = x_0 \pm \frac{\alpha\Delta}{2k\mathrm{d}}. \tag{41}$$

From Eq. (41) it follows that two C-lines of opposite handedness are located symmetrically around x_0. Thus we conclude that on changing the polarization angle α from zero to a finite value, each dark line unfolds into a triplet of polarization singularities, namely an *L-line with two C*-lines

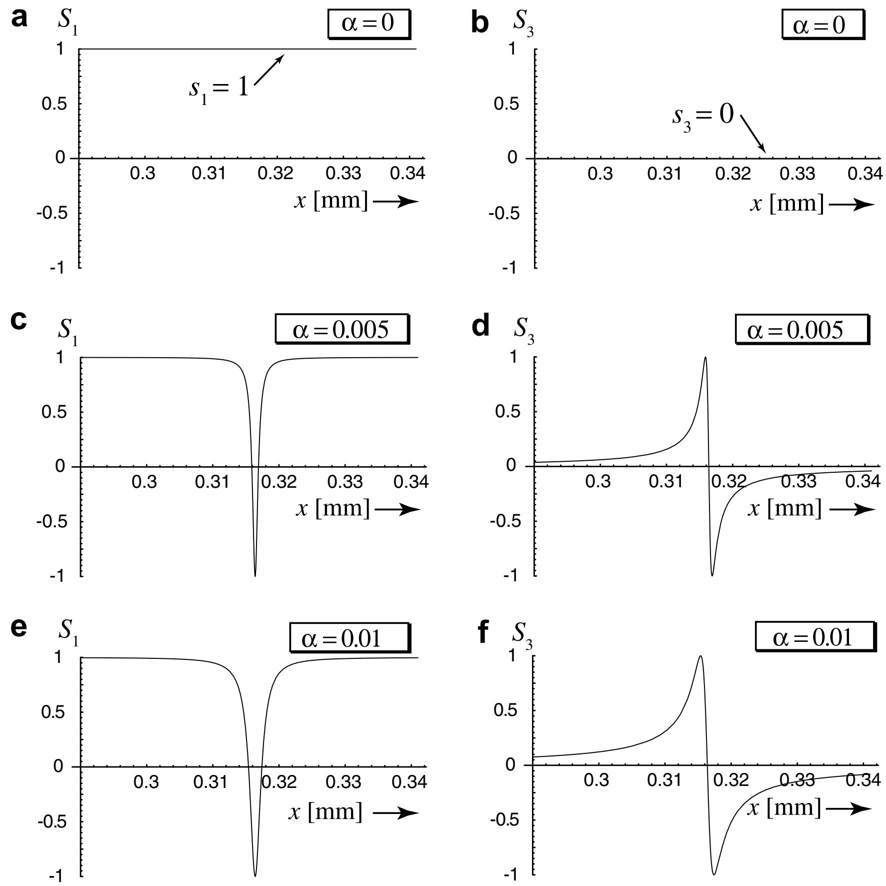

Fig. 3. The Stokes parameters s_1 and s_3 as a function of position for selected values of the orientation angle α. In this example $\lambda = 632.8$ nm, $\Delta = 2$ m, and $2d = 2$ mm.

of opposite handedness on either side. It is to be noted that according to Eq. (41) the polarization singularities move away from each other when the angle α is increased, but they remain in existence. In other words, they are structurally stable. We emphasize that, since our system is approximately invariant along the y-direction, we are dealing with C-lines rather than the generically occurring C-points [31–33]. Also, this unfolding is reminiscent of a similar process in crystal optics [34,35].

An example of the unfolding process is shown in Fig. 3. There the behavior of the Stokes parameters s_1 and s_3 in the vicinity of the dark line at x_0 is depicted for selected values of the angle α. In calculating the plots the exact expressions for the factors K_j are used, rather than their approximate forms. In Fig. 3a and b, the case of two perfectly aligned directions of polarization ($\alpha = 0$) is shown. It is seen that $s_1 = 1$ and $s_3 = 0$ over the entire range, i.e. the field is everywhere linearly polarized along the x-direction. Fig. 3c and d show the state of polarization when the two polarization directions are under an angle $\alpha = 0.005$ with each other. Precisely at the location of the vanished dark line (at $x_0 = 0.316$ mm) an L-line with $s_1 \approx -1$ has appeared. Also, the behavior of the Stokes parameter s_3 has drastically changed: to the left of x_0 a right-handed C-line ($s_3 = 1$) has appeared, together with a left-handed C-line ($s_3 = -1$) to the right of x_0. In Fig. 3e and f the same Stokes parameters are shown for a larger value of the angle α. It is seen that the triplet of polarization singularities still occurs, but with the two C-lines further separated from each other, as is suggested by Eq. (41). Also, the behavior of the parameters in the neighborhood of the former dark line has become smoother. In all numerical calculations it was found that $|s_2| < 0.01$.

The effects predicted in this paper can be produced, for example, by using a setup described by Thompson and Wolf [36] that produces a field with a variable spectral degree of coherence. By adding two polarizers, the angle α between the two directions of polarization of the incident fields can be controlled.

4. Conclusions

An analysis of Young's interference experiment for the case when two correlated beams of identical linear polarization are used was presented. It was found that correlation singularities are always present. When the two beams become fully coherent and co-phasal, the correlation singularities annihilate in a cross-pair wise manner, and dark lines are created. On changing the polarization directions with respect to each other, each dark line unfolds into a triplet of polarization singularities.

Acknowledgement

RWS acknowledges support by the National Science Foundation under CAREER Grant No. 0239265. TDV thanks Professor Michael Berry for robust discussions.

References

[1] T. Young, Phil. Trans. R. Soc. Lond. 94 (1804) 1.
[2] T. Young, A Course of Lectures on Natural Philosophy and the Mechanical Arts, vol. 2, Johnson, London, 1807.
[3] M. Born, E. Wolf, Principles of Optics: Electromagnetic Theory of Propagation Interference and Diffraction of Light, seventh ed., Cambridge University Press, Cambridge, 1999.
[4] H.F. Schouten, T.D. Visser, E. Wolf, Opt. Lett. 28 (2003) 1182.
[5] G.S. Agarwal, A. Dogariu, T.D. Visser, E. Wolf, Opt. Lett. 30 (2005) 120.
[6] H.F. Schouten, N. Kuzmin, G. Dubois, T.D. Visser, G. Gbur, P.F.A. Alkemade, H. Blok, G.W. 't Hooft, D. Lenstra, E.R. Eliel, Phys. Rev. Lett. 94 (2005) 053901.
[7] N. Kuzmin, G.W. 't Hooft, E.R. Eliel, G. Gbur, H.F. Schouten, T.D. Visser, Opt. Lett. 32 (2007) 445.
[8] D.G. Fischer, T.D. Visser, J. Opt. Soc. Am. A 21 (2004) 2097.
[9] D.M. Palacios, I.D. Maleev, A.S. Marathay, G.A. Swartzlander Jr., Phys. Rev. Lett. 92 (2004) 143905.
[10] G.A. Swartzlander Jr., J. Schmit, Phys. Rev. Lett. 93 (2004) 093901.
[11] W. Wang, Z. Duan, S.G. Hanson, Y. Miyamoto, M. Takeda, Phys. Rev. Lett. 96 (2006) 073902.
[12] H.F. Schouten, G. Gbur, T.D. Visser, E. Wolf, Opt. Lett. 28 (2003) 968.
[13] M. Mujat, A. Dogariu, E. Wolf, J. Opt. Soc. Am. A 21 (2004) 2414.
[14] H. Roychowdhury, E. Wolf, Opt. Commun. 252 (2005) 268.
[15] T. Setälä, J. Tervo, A.T. Friberg, Opt. Lett. 31 (2006) 2669.
[16] M.S. Soskin, M.V. Vasnetsov, in: E. Wolf (Ed.), Progress in Optics, vol. 42, Elsevier, Amsterdam, 2001.
[17] J.F. Nye, Natural Focusing and Fine Structure of Light, IOP Publishing., Bristol, 1999.
[18] M.V. Berry, M.R. Dennis, Proc. R. Soc. Lond. A 457 (2001) 141.
[19] M.R. Dennis, Opt. Commun. 213 (2002) 201.
[20] I. Freund, A.I. Mokhun, M.S. Soskin, O.V. Angelsky, I.I. Mokhun, Opt. Lett. 27 (2002) 545.
[21] A.I. Mokhun, M.S. Soskin, I. Freund, Opt. Lett. 27 (2002) 995.
[22] I. Freund, Opt. Commun. 201 (2002) 251.
[23] M.S. Soskin, V. Denisenko, I. Freund, Opt. Lett. 28 (2003) 1475.
[24] R.W. Schoonover, T.D. Visser, Opt. Express 14 (2006) 5733.
[25] G. Gbur, T.D. Visser, E. Wolf, J. Opt. A: Pure Appl. Opt. 6 (2004) S239.
[26] L. Mandel, E. Wolf, Optical Coherence and Quantum Optics, Cambridge University Press, Cambridge, 1995.
[27] G. Gbur, T.D. Visser, E. Wolf, Opt. Commun. 239 (2004) 15.
[28] L. Basano, P. Ottonello, Phys. Rev. Lett. 94 (2005) 173901.
[29] D. Ambrosini, F. Gori, D. Paoletti, Opt. Commun. 254 (2005) 30.
[30] J.D. Jackson, Classical Electrodynamics, Second ed., Wiley, New York, 1975.
[31] G.V. Bogatyryova, Ch.V. Felde, P.V. Polyanskii, S.A. Ponomarenko, M.S. Soskin, E. Wolf, Opt. Lett. 28 (2003) 878.
[32] M.S. Soskin, P.V. Polyanskii, O.O. Arkhelyuk, New J. Phys. 6 (2004) 196.
[33] G.V. Bogatyryova, K.V. Felde, P.V. Polyanskii, M.S. Soskin, Opt. Spectro. 97 (2004) 782.
[34] F. Flossmann, U.T. Schwarz, M. Maier, M.R. Dennis, Phys. Rev. Lett. 95 (2005) 253901.
[35] F. Flossmann, U.T. Schwarz, M. Maier, M.R. Dennis, Opt. Express 14 (2006) 11402.
[36] B.J. Thompson, E. Wolf, J. Opt. Soc. Am. 47 (1957) 895.